Int J. Heat Mass Transfer. Vol. 10, pp. 1709–1716. Pergamon Press Ltd. 1967. Printed in Great Britain

DIRECTIONAL EMITTANCE OF AN ELECTRIC NONCONDUCTOR AS A FUNCTION OF SURFACE ROUGHNESS AND WAVELENGTH*

K. E. TORRANCE† and E. M. SPARROW‡

(*Received* 28 *September* 1966 *and in revised form* 12 *June* 1967)

Abstract—Directional distributions of thermal radiation emitted from a succession of smooth to roughened surfaces of an electric nonconductor have been measured monochromatically. The test material was an aluminum oxide ceramic, while the ranges of surface roughness and wavelength respectively extended from 0·26 to 3·8 μ and from 4 to 12 μ. The directional emittance distributions, normalized by the corresponding normal emittances, exhibit a strong dependence on wavelength. Moreover, the normalized emittance distributions are not monotonically ordered with wavelength. At a given wavelength, the emittance distribution tends to approach toward the diffuse limit as the surface roughness increases. However, the rate of approach is not rapid, and if the diffuse limit is to be achieved at all, surfaces of very substantial roughness will be required. Comparisons were made between the experimental results and the predictions of electromagnetic theory in those wavelength ranges in which the optical constants are available. Good agreement was found both in the general trend with wavelength as well as for the detailed directional distributions for the highly polished test surface.

NOMENCLATURE

e, radiant energy;
i, radiant intensity, equation (2);
k, extinction coefficient;
n, index of refraction.

Greek symbols
Δ, detector output;
$\epsilon(\theta)$, monochromatic directional emittance;
θ, angle of emission measured from surface normal [degrees];
λ, wavelength [μ];
μ, micron [10^{-6} m];
σ, root-mean-square surface roughness [μ];
ω, solid angle [sr].

* This paper is based on work done at the Heat Transfer Laboratory, Department of Mechanical Engineering, University of Minnesota, Minneapolis, Minnesota.

† Research Associate at the National Bureau of Standards from the Factory Mutual Engineering Corporation, Norwood, Massachusetts.

‡ University of Minnesota, Minneapolis, Minnesota.

1. INTRODUCTION

THE DIRECTIONAL distribution of the monochromatic thermal radiation emitted from a perfectly smooth surface of a homogeneous solid can be calculated from the Fresnel equation [1]. However, the surfaces of real engineering materials depart by various degrees from the ideal conditions postulated by the Fresnel model. The effect of surface roughness on the monochromatic directional emission characteristics of metallic surfaces has already been experimentally examined [2–4]. On the other hand, within the knowledge of the present authors, experimental information on the effects of roughness and wavelength on the directional emittance distribution has yet to be reported for nonmetals. It was to provide basic information of this type that the present study was initiated.

The material employed in this investigation was an aluminum oxide ceramic from which were prepared test specimens of varying surface roughness. Directional emittance measurements

5Q

were made for surface roughnesses ranging from 0·26 to 3·8 μ over a wavelength range extending from 4 to 12 μ. The test specimens were heated to 300°F, and the emitted radiation was collected in a small solid angle at inclination angles (relative to the surface normal) ranging from 0 to 85°. The measured results are displayed so as to highlight the separate effects of surface roughness and of wavelength. Comparisons are made with the predictions of the Fresnel equation.

2. APPARATUS AND MEASUREMENT TECHNIQUE

A schematic diagram of the experimental apparatus is shown in Fig. 1. A test specimen A (normal $\hat{n}$) is held against an electrically heated copper block B. The assembly consisting of the specimen and the heater can be rotated about an axis lying in the plane of the specimen surface and perpendicular to the plane of the figure. A water-cooled enclosure C, with blackened walls, surrounds the specimen-heater assembly. A shaft extending through the walls of the enclosure C facilitates external adjustment of the zenith angle of emission θ. A viewing port in the enclosure C permits radiation leaving the test specimen at a pre-selected angle to be collected by mirror E and focused on the entrance slit of the monochromator F. A water-cooled blackbody cavity D can be positioned in front of the viewing port in C to permit measurements which facilitate the accounting of the background radiation within C.

The monochromator F is a Perkin–Elmer model 99 equipped with a sodium chloride prism and a thermocouple detector. The mirror E is a first-surface aluminum-coated spherical mirror. When viewed respectively from the specimen surface and the spectrometer entrance slit, the mirror subtends solid angles of $\pi/1764$ and $\pi/1024$ sr. Alignment of the optical components of the apparatus was achieved by placing a light source G at the exit slit of the monochromator, thus essentially reversing the radiation path.

Thermocouples were imbedded in the surface of each test specimen as well as in the surface of the heated copper block. Additional thermocouples sensed the wall temperatures of the

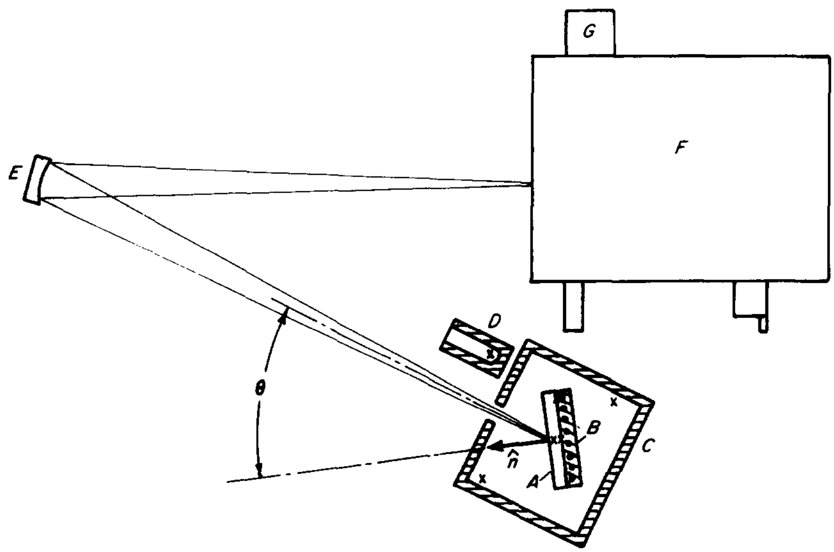

FIG. 1. Schematic diagram of experimental apparatus.

cavity C and the blackbody D. Thermocouple locations are indicated with "×" symbols in Fig. 1. The thermocouples were fabricated from calibrated chromel–alumel wire, 30 gage. The thermocouple emf's were read to an accuracy of $\pm 0{\cdot}2$ degF with a portable potentiometer.

The test material was an aluminum oxide ceramic* with a nominal composition of 95% aluminum oxide and 5% magnesium aluminum silicate. Two test specimens with the same surface dimensions (2 by 6 in) but of different thickness ($\frac{5}{16}$ and $\frac{5}{8}$ in) were employed. The two thicknesses were used to establish that the measured results are independent of the radiation properties of the backing material (i.e. the copper heating block).

The as-arrived RMS surface roughness of the two specimens was 1·7 μ. After emittance measurements for this surface condition had been performed, the surface of the $\frac{5}{16}$-in thick specimen was ground by a standard optical technique to achieve a succession of other values of the RMS surface roughness σ as listed in the legend of Fig. 3. The 0·26, 0·37 and 3·8 μ roughnesses were achieved, respectively, by polishing, grinding with 1200 grit silicon carbide, and grinding with 80 grit silicon carbide.

Polishing was performed with cerium oxide on a felt pitch lap. The residual roughness of 0·26 μ on the polished surface is due to the polycrystalline structure. The 80 grit silicon carbide was the coarsest grit which would provide an isotropic roughness. Some 40 grit material was tried, but the resulting surface texture was wavy and nonuniform. All test surfaces were subjected to ultrasonic cleaning and microscopic examination. The surface roughness was measured with the aid of a stylus profilometer†.

The directional emittance $\epsilon(\theta)$ was measured relative to that in the direction of the surface normal $\epsilon(0°)$. This latter quantity, the *normal* emittance, has been found by experiment to be only negligibly affected by surface roughness [5, 6]. The monochromatic normal emittance $\epsilon(0°)$ can thus be taken from the literature [7–9] and was not determined as part of this study.

The aforementioned ratio of emittances can be expressed as a ratio of radiant intensities

$$\frac{\epsilon(\theta)}{\epsilon(0°)} = \frac{i(\theta)}{i(0°)} \tag{1}$$

where, in turn,

$$\left.\begin{aligned} i(\theta) &= \frac{\mathrm{d}e(\theta)}{\mathrm{d}\omega \cos\theta}, \\ i(0°) &= \frac{\mathrm{d}e(0°)}{\mathrm{d}\omega} \end{aligned}\right\} \tag{2}$$

in which de is the emitted radiant energy per unit time and unit *surface* area that is contained within the solid angle dω. The quantity d$e/\cos\theta$ is the rate of emitted radiation per unit projected area in the direction θ.

The experimental arrangement is such that the projected area and dω remain constant as the zenith angle θ is varied. Therefore, in the absence of background radiation effects, the output of the detector is proportional to the intensity of the emitted radiation.

However, the radiant energy leaving the surface includes both emitted radiation and reflected radiation, the latter originating at the blackened walls of the enclosure C of Fig. 1. The effect of such background radiation on the emittance measurement has been analyzed [10] for the case of total radiation, and a parallel development can be carried through for monochromatic radiation. On the basis of such a development, one finds

$$\frac{\epsilon(\theta)}{\epsilon(0°)} = \frac{\Delta(\theta) - \Delta_r}{\Delta(0°) - \Delta_r} \tag{3}$$

for a given wavelength and specimen surface temperature. In this expression, $\Delta(\theta)$ and $\Delta(0°)$ respectively denote the detector outputs when the specimen surface is viewed at $\theta = \theta$ and

* Honeywell, Inc. type A-203 Alumina, grain size 5–10 μ, porosity (closed) about 5 per cent.

† Micrometrical type QB with a stylus tip radius of 0·0005 in and a roughness-width cut-off length of 0·030 in.

$\theta = 0°$. Δ_r represents the detector output when the monochromater views the blackbody D, when the latter is positioned in front of the viewing port of the enclosure C and is maintained at the same temperature as the enclosure walls.

3. RESULTS AND DISCUSSION

The experimental results obtained by applying equation (3) are shown in Figs. 2 and 3 with the emission angle θ as abscissa. The first of these figures applies for a particular surface roughness σ and highlights the effect of variations of the wavelength λ. The second of these figures consists of three graphs, each corresponding to a given wavelength λ. In each of these graphs, the surface roughness σ appears as the curve parameter. The information shown in Figs. 2 and 3 pertains to a surface temperature of approximately 300°F. In all cases, the directional emittance decreases monotonically with increasing values of the zenith angle θ. This is consistent with the predictions of electromagnetic theory for electric nonconductors as well as with prior measurements of total emission from surfaces of unspecified roughness [11].

The curves in Fig. 2 portray the directional emittance distributions for a particular surface roughness as the wavelength λ ranges from 4 to 12 μ. The data in the figure apply for the as-arrived surface roughness $\sigma = 1{\cdot}7$ μ. The broken lines* and open symbols in column A of the legend denote data for the $\frac{5}{16}$-in thick specimen, while the darkened symbols in column B denote data for the $\frac{5}{8}$-in thick specimen. Good agreement between the two sets of data suggests that both specimens are sufficiently thick to be considered opaque, thereby indicating that the measured results are independent of the radiation properties of the backing material.

The curves in Fig. 2 display a significant trend with wavelength. In the type of presentation employed here, a perfectly diffuse emitter (i.e. one which obeys Lambert's cosine law) would have a constant value of $\epsilon(\theta)/\epsilon(0°) = 1$. As the wavelength increases from 4 to 8 μ, the experimental curves tend to approach the diffuse distribution. This trend with increasing wavelength can be related to a decreasing index of refraction in this range as will be discussed in a subsequent paragraph. A further increase in wavelength beyond 8 μ, however, reveals an opposite trend characterized by an increasing departure from the diffuse model. Inasmuch as the optical constants are unavailable beyond 8 μ, it is not possible to relate this trend to variations in the constants.

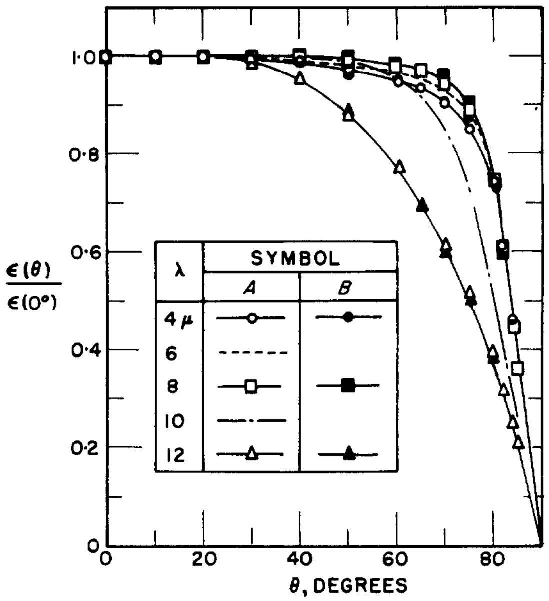

FIG. 2. Effect of wavelength (λ) on the directional emittance distributions, surface roughness $\sigma = 1{\cdot}7$ μ. The symbols in columns A and B denote data on $\frac{5}{16}$ and $\frac{5}{8}$-in thick specimens, respectively.

Figure 3 consists of three separate graphs. Each of the graphs displays the effect of varying surface roughness at a particular wavelength ($\lambda = 4$, 8, or 12 μ). The data in Fig. 3 were obtained on the $\frac{5}{16}$-in thick specimen for surface roughnesses ranging from 0·26 μ (highly polished) to 3·8 μ. Data from Fig. 2 for the as-arrived surface roughness ($\sigma = 1{\cdot}7$ μ) are also included.

* The data points for the measurements at $\lambda = 6$ and 10 μ were omitted to preserve clarity.

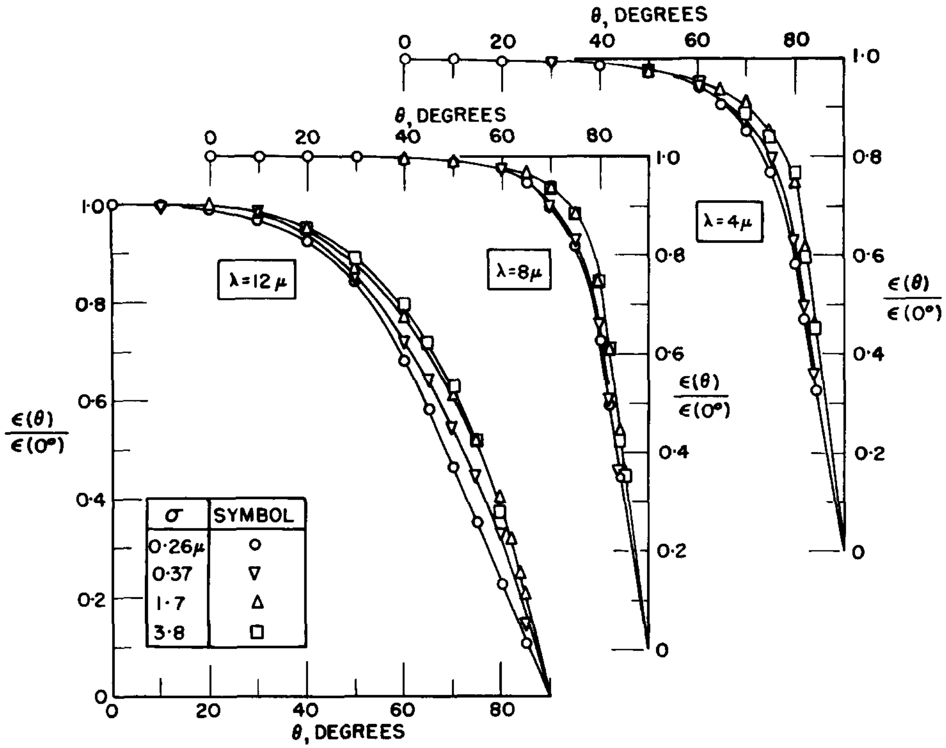

FIG. 3. Effect of surface roughness (σ) on the directional emittance distributions, wavelength $\lambda = 4$, 8 and 12 μ.

The significant feature shown in Fig. 3 is the manner in which the measured distributions approach the diffuse limit with increasing surface roughness. For each wavelength, the lowest curve corresponds to the polished surface. As the surface roughness is increased, the directional distributions depart from that for the polished surface and tend toward the diffuse limit. However, it is interesting to observe that the difference between the distributions corresponding to $\sigma = 1{\cdot}7$ and $3{\cdot}8$ μ is very small or even indistinguishable, compared with that between $\sigma = 0{\cdot}26$ and $1{\cdot}7$ μ. Therefore, if the diffuse limit is actually to be achieved, surface roughnesses of magnitudes substantially greater than those of this investigation will be required. The experience of the present authors suggests that it may be difficult to achieve such roughness magnitudes while maintaining the isotropy of the surface.

It is also interesting to compare the relative effects of surface roughness and wavelength on the directional distributions. From an overall view, it appears that the changes with surface roughness (at a given wavelength) are substantially less than are those with wavelength (at a given surface roughness) in the range $\lambda = 8$–12 μ.

As was noted earlier, the directional emittance of an optically smooth surface can be calculated from the Fresnel equation. This equation is derived from electromagnetic theory and yields the directional emittance (or the specular reflectance) in terms of the optical constants of the solid [1]. The required constants are the index of refraction, n, and the extinction coefficient, k. For dielectrics, the extinction coefficient is usually assumed to be zero, except near absorption bands.

The refraction indices for synthetic sapphire* at $\lambda = 4$ and $8\ \mu$ ($n = 1{\cdot}68$ and $n \simeq 1{\cdot}3$, respectively) were obtained from [12]. The value at $\lambda = 4\ \mu$ could be read directly, whereas that at $\lambda = 8\ \mu$ required a moderate extrapolation. Using these n values, directional emittance distributions have been calculated from the Fresnel equation and are compared with the experimental data for the polished surface ($\sigma = 0{\cdot}26\ \mu$) in Fig. 4. In the range of θ between 0 and 75°, excellent agreement between the analytical and experimental results is in evidence. For larger values of θ, the calculated results are somewhat above the experimental data. Inasmuch as the wavelength dependent trends of Fig. 2 also apply to the polished surface, it follows that the results of Fig. 2 are in qualitative accord with electromagnetic theory in the wavelength range from 4 to 8 μ.

A similar comparison of theory with experiment at $\lambda = 12\ \mu$ cannot be made owing to the lack of information on the optical constants in this region. The available data on the index of refraction are restricted to the near infrared [12], $\lambda \leqslant 5{\cdot}6\ \mu$, and to the far infrared [13, 14], $\lambda \geqslant 100\ \mu$. The index of refraction in both regions decreases with increasing wavelength; the magnitude in the near infrared is on the order of 1·6, whereas in the far infrared it is about 3·1. Thus, extrapolation to $\lambda = 12\ \mu$ is highly questionable. In addition, the region between 10 and 20 μ contains absorption

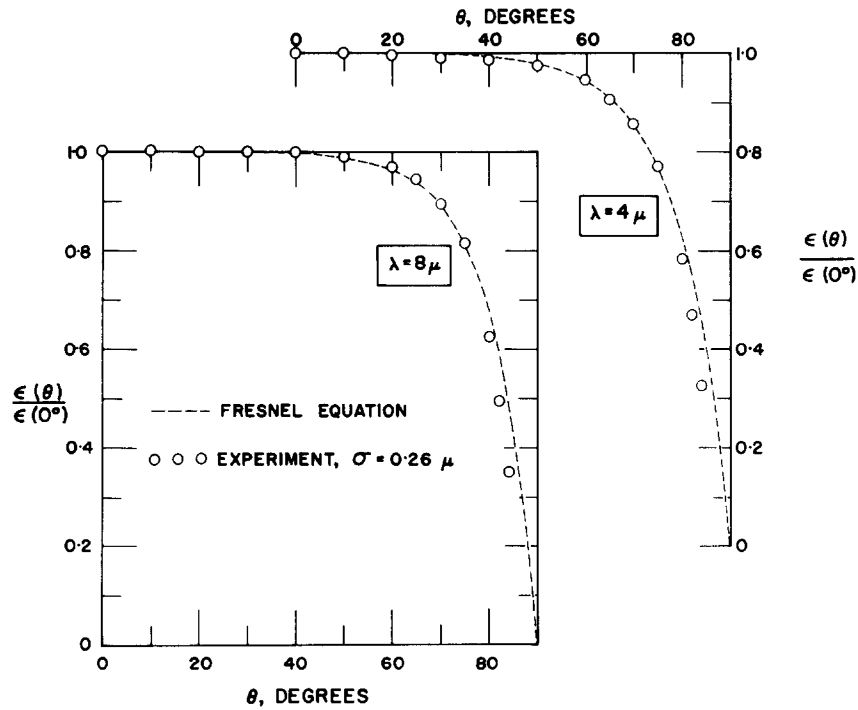

FIG. 4. Theoretical and experimental directional emittance distributions, wavelength $\lambda = 4$ and $8\ \mu$. Experimental data for polished surface, surface roughness $\sigma = 0{\cdot}26\ \mu$.

*Sapphire is a mineral variety of aluminum oxide.

bands, thus requiring a knowledge of the extinction coefficient k, which is presently unavailable.

4. CONCLUDING REMARKS

The significant findings of this investigation may be summarized as follows:

1. The directional emittance distributions for a given surface roughness, normalized by the normal emittance, exhibit a strong dependence on wavelength. Moreover, the normalized distributions are not arranged in monotonic order according to wavelength. In the range of wavelengths in which the optical constants are available, the trend with wavelength is in agreement with that predicted by electromagnetic theory.
2. At a given wavelength, the emittance distribution tends to approach toward the diffuse limit with increasing surface roughness. However, the approach is not very rapid, suggesting that if the limit is reached at all, it will only be for very substantial surface roughness.
3. When the optical constants are known or can be reasonably estimated, the normalized emittance distributions for the polished surface are in good agreement with electromagnetic theory.

ACKNOWLEDGEMENT

The support of the National Aeronautics and Space Administration under Grant NsG 137-61 is gratefully acknowledged.

REFERENCES

1. E. M. Sparrow and R. D. Cess, *Radiation Heat Transfer*, p. 68. Wadsworth, Belmont, Calif. (1966).
2. R. Hase, Emission von Aluminum und seinen Legierungen, *Zeitschrift für technische Physik* **13**, 145–155 (1932).
3. D. K. Edwards and I. Catton, Radiation characteristics of rough and oxidized metals, in *Advances in Thermophysical Properties at Extreme Temperatures and Pressures*, pp. 189–199. Am. Soc. Mech. Engrs, New York (1965).
4. R. E. Rolling, A. I. Funai and J. R. Grammer, Investigation of the effect of surface condition on the radiant properties of metals, Lockheed Missiles and Space Company, Tech. Rep. No. AFML-TR-64-363 (AD No. 466662) (November 1964).
5. J. C. Richmond, Effect of surface roughness on emittance of non-metals, *J. Opt. Soc. Am.* **56**, 253–254 (1966).
6. R. E. Gannon and B. Linder, Effect of surface roughness and porosity on emittance of alumina, *J. Am. Ceram. Soc.* 47, 592–593 (1964).
7. H. H. Blau Jr., J. B. Marsh, W. S. Martin, J. R. Jasperse and E. Chaffee, Infrared spectral emittance properties of solid materials, Arthur D. Little, Inc., Rep. No. AFCRL-TR-60-416 (AD No. 248276), (October 1960).
8. R. C. Folweiler and W. J. Mallio, Thermal radiation characteristics of transparent, semi-transparent, and translucent materials under non-isothermal conditions, Lexington Laboratories, Inc., Rep. No. ASD-TDR-62-719 Part II (AD No. 607742) (June 1964).
9. H. E. Clarke and D. G. Moore, Method and equipment for measuring thermal emittance of ceramic oxides from 1200° to 1800°K, *Symposium on Thermal Radiation of Solids*, edited by S. Katzoff, pp. 241–257. NASA SP-55 (Air Force ML-TDR-64-159) (1965).
10. E. R. G. Eckert, J. P. Hartnett and T. F. Irvine Jr., Measurement of total emissivity of porous materials in use for transpiration cooling, *Jet Propul.* **26**, 280–282 (1956).
11. E. R. G. Eckert and R. M. Drake Jr., *Heat and Mass Transfer*, 2nd edn., p. 377. McGraw-Hill, New York (1959).
12. I. H. Malitson, F. V. Murphy Jr. and W. S. Rodney, Refractive index of synthetic sapphire, *J. Opt. Soc. Am.* **48**, 72–73 (1958).
13. E. V. Loewenstein, Optical properties of sapphire in the far infrared, *J. Opt. Soc. Am.* **51**, 108–112 (1961).
14. S. Roberts and D. D. Coon, Far-infrared properties of quartz and sapphire, *J. Opt. Soc. Am.* **52**, 1023–1029 (1962).

Résumé—Les distributions dans différentes directions du rayonnement thermique émis à partir d'une série de surfaces, allant d'un aspect lisse à un aspect rugueux, d'un corps non conducteur de l'électricité ont été mesurées pour une longueur d'onde déterminée. Le matériau essayé était une céramique en oxyde d'aluminium, tandis que les gammes de rugosité de surface et de longueur d'onde s'étendaient respectivement de 0,26 à 3,8 microns et de 4 à 12 microns. Les distributions de la brillance rapportée à la brillance normale correspondante, dépendent d'une façon importante de la longueur d'onde.

De plus, les distributions de brillance relative ne varient pas d'une façon monotone avec la longueur d'onde. Pour une longueur d'onde donnée, la distribution de brillance tend à s'approcher vers la limite de l'émission diffuse lorsque la rugosité de la surface augmente. Cependant, la vitesse d'approche n'est pas rapide, et si la limite de l'émission diffuse doit être atteinte d'une façon quelconque, des surfaces avec une rugosité très considérable seraient nécessaires. On a établi des comparaisons entre les résultats expérimentaux et les prédictions de la théorie électromagnétique dans ces gammes de longueurs d'onde où les constantes optiques son disponibles. On a trouvé un bon accord avec la tendence générale de varia tion avec la longueur d'onde aussi bien que pour les distributions en fonction de la direction qui ont été décrites en détail dans le cas où la surface d'essai est fortement polie.

Zusammenfassung—Die Richtungsverteilungen thermischer Strahlung, wie sie eine Reihe von glatten bis rauhen Oberflächen eines elektrischen Isolators emittieren, wurden monochromatisch gemessen. Das Versuchsmaterial bestand aus Aluminiumoxid mit einem Rauhigkeitsbereich von 0,26 bis 3,8 μ bei Wellenlängen von 4 bis 12 μ. Die Richtungsverteilung der Emission, bezogen auf die entsprechende Normalemission, zeigt eine starke Abhängigkeit von der Wellenlänge. Ausserdem lassen sich die Normalverteilungen der Emission nicht monoton nach der Wellenlänge ordnen. Bei gegebener Wellenlänge nähert sich die Emissionsverteilung dem Diffusionsgrenzwert, wenn die Oberflächenrauhigkeit zunimmt. Allerdings erfolgt die Annäherung nicht schnell und falls der diffuse Grenzwert überhaupt erreicht wird, sind dazu Oberflächen beträchtlicher Rauhigkeit nötig. Für die Bereiche, in welchen die optischen Konstanten vorlagen, wurden Vergleiche zwischen den Versuchsergebnissen und Berechnungen nach der elektromagnetischen Theorie angestellt. Gute Übereinstimmung ergab sich sowohl beim allgemeinen Verlauf entsprechend der Wellenlänge als auch bei speziellen Richtungsverteilungen für hochwertige Versuchsflächen.

Аннотация—Монохроматически измерялись направленные распределения теплового излучения с гладких и шероховатых поверхностей электроизолятора. Исследуемым материалом служила керамика из окиси алюминия, при этом шероховатость поверхности и длина волны изменялсиь от 0,26 до 3,8 микрон и от 4 до 12 микрон, соответственно. Направленные распределения излучения, нормализованные соответствующим обычным излучением, показывают сильную зависимость от длины волны. Более того, нормализованные распределения излучения линейно не зависят от длины волны. Для данной длины волны распределение излучения стремится к диффузионному пределу с увеличением шероховатости поверхности. Однако, скорость приближения не велика, и если вообще нужно достичь диффузионного предела, то требуются поверхности с очень большой шероховатостью. Сравнивались экспериментальные результаты с расчетами, сделанными на основании электромагнитной теории в тех диапазонах, в которых имеются оптические постоянные. Найдено хорошее соответствие как с длиной волны, так и с данными по направленному распределению в случае хорошо отпалированной поверхности.